A New Approach to Horizontal Backfill Exposure Analysis

Matthew Helinski

MineFill Services, Sydney, NSW, Australia, matth@minefill.com

Abstract

Historically the limit equilibrium solutions by Mitchell and Roettger (1989) have been used when specifying backfill strengths for horizontal exposures. While these solutions have proven useful for small spans, where ground support is included (eg, in underhand cut and fill mining), experience shows this approach to underestimate dilution in larger underhand stoping applications with cemented paste and hydraulic fill, and overestimate the strength required to prevent catastrophic failure (ie, achieve stability, while permitting some dilution).

Persistent, cohesionless, horizontal 'cold/flow' joints, which form during the hydraulic deposition process are expected to be controlling the horizontal exposure mechanism. After incorporating the influence of these joints into discontinuum numerical analysis, this model is shown to provide a more reasonable representation of the relationship between dilution and strength during horizontal exposures. Based on the mechanics revealed from the numerical output two new analytical modes are proposed for representing the horizontal exposure behaviour. The first is based on Voussoir beam theory and relates depth of overbreak (or dilution) to backfill strength, while the second provides a model for estimating the strength below which catastrophic, uncontrolled caving would occur. Finally, the analytical solutions suggest horizontal exposures to be largely independent of tensile strength. This is verified through a numerical sensitivity study.

Key words: cemented backfill, strength requirements, horizontal exposures, numerical analysis, field studies, analytical solutions

Introduction

As miners gain confidence in the quality of hydraulically placed backfill (cemented paste or hydraulic fill) increased expectations about the exposure performance has enabled incredible increases in efficiency of many underground mines. This is most notable in weak ground conditions where the underhand retreat stope extraction sequence with backfill is gaining increased popularity. While the extraction of ore from immediately beneath cemented fill often requires high backfill strengths, this strategy delivers very significant benefits, most notably through improved geotechnical stress conditions, earlier access to stoping ore, elimination of floor dilution, and often an opportunity to reduce waste development.
In recent times, the author has been involved with many operations where horizontal fill exposures exceed 15 m as well as a number of sites considering the application of this method for stopes with spans exceeding 25 m. The author's experience has shown that, when applied in this context, existing analytical solutions (eg, Mitchell and Roettger, 1989) do not properly address the critical failure mechanisms and mislead the miners in terms of underestimating dilution and overestimating strength requirements.

This paper uses a combination of numerical analysis and field observations to develop an improved understanding about the mechanics that control horizontal cemented backfill exposure stability, before drawing on two existing analytical solutions to provide simplified solutions for better characterising this behaviour.

Traditional Approach to Horizontal Exposure Design

Traditionally horizontal backfill exposures have been designed based on the analytical solutions developed by Mitchell and Roettger (1989) and later applied by many others, including Pakalnis et al. (2005). This work presents a series of analytical solutions, based on beam theory and limit equilibrium, to represent different failure mechanisms; these solutions are then verified through geotechnical centrifuge testing. The derived solutions and associated functions were neatly summarised by Pakalnis et al. (2005) (Figure 1).

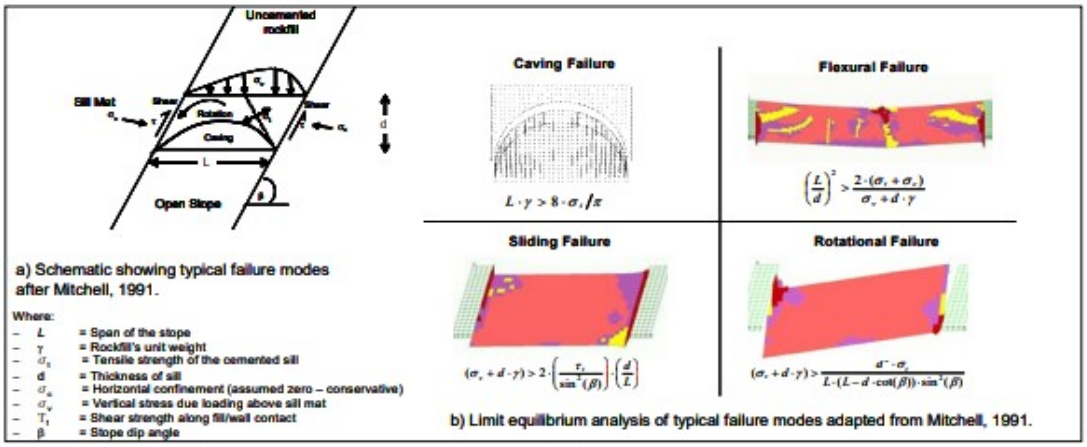

Figure 1. Limit equilibrium solutions for horizontal backfill exposures by Pakalnis et al. (2005), as adapted from Mitchell (1989).

These solutions were originally developed for small horizontal backfill exposures, typically encountered while mining using the underhand cut and fill method. These solutions can be useful in this context, where shorter fill spans are bound using ground support, or in the application of mechanically placed backfill. However, experience has shown these solutions to perform poorly in larger non-man entry applications with hydraulically deposited backfill (ie, paste or hydraulic fill). Examples of this at two Australian mine sites are shown in Figure 2a and b, where the images show two cavity monitoring surveys (Figure 2a shows both long and cross section views). The overlying stopes were extracted and then refilled first, before extracting the underlying voids. In Figure 2b, the underlying left-hand side (LHS) stope was extracted and filled to floor height, before extracting the right-hand side (RHS) stope. The overlap of the two surveys represents fill over break.

Also shown beneath each figure is the exposure dimension, fill strength design (in accordance with solutions based on Mitchell and Roettger (1989)), actual fill strength (based on plant quality control testing), and quantity of dilution. These calculations assume the tensile strength to be equal to the fill cohesive strength, as verified through testing. This equates to a UCS/tensile strength ratio of approximately 4, which aligns with data presented by Grabinsky et al. (2022). Figure 2a shows that, even though the actual fill strength exceeds both critical failure mechanisms (ie, flexure and caving) from Mitchell and Roettger (1989), exposure still results in over 1500 m^3 of backfill dilution. Conversely, Figure 2b shows that even though the backfill does not achieve the strength required to resist flexural failure, the flexural failure mechanism does not propagate to catastrophic failure. Rather, in both cases a (stable) "arch" shaped failure profile forms. This contradicts the flexural failure mechanism, which suggests that the loss of beam thickness (ie, reduction in the "d" term) due to the noted dilution would further increase instability. Furthermore, if the "caving" is creating the observed dilution, the strength

requirements are grossly underestimated by the proposed relationship as the *in situ* strength is expected to provide a FoS of 5.4 and 3.4 against this mechanism.

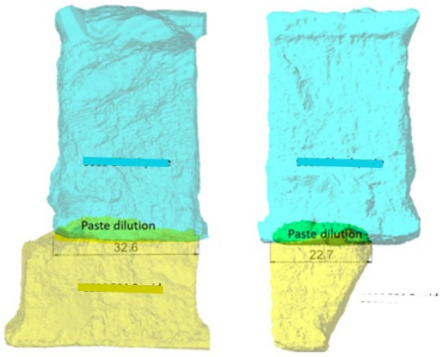

Exposure Dims. – 32 x 22 m - 50 m height
Fill Strength – 2547 kPa
Mitchell Estimate – Flexure (1,313 kPa), Caving (474 kPa).
Dilution – 1563 m^3

(a)

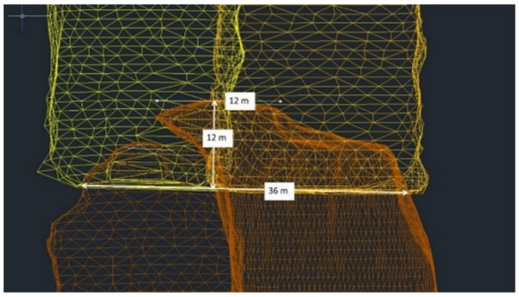

Exposure Dims. – 36 x 20 m - 25 m height
Fill Strength – 1,400 kPa
Mitchell Estimate – Flexure (1,823 kPa), Caving (412 kPa)
Dilution – 5184 m^3

(b)

Figure 2a and b. Examples of horizontal backfill exposures at different sites.

Horizontal Exposure Failure Mechanism

The reason for the behaviour observed in Figure 2 are expected to be a result of 'cold' or 'flow' jointing. Photographs showing this cold/flow jointing in paste backfill at three different mines is presented in Figure 3. While these three sites are totally different backfill systems, the one common feature of each is that the presented section was placed in a continuous pour (ie, the jointing is not a consequence of fill stoppages). The objective of this paper is to discuss the implications of these cold joints rather than the mechanism, but it should be noted that these three sites represent a range of high and low yield stress paste, with varying binder content and vertical rate of rise.

Figure 3. Cold/flow jointing in two different paste backfill masses.

Based on experience, the jointing shown in Figure 3 is observed at most sites and, while the author has no firm evidence to verify the cause, the jointing is expected to occur because of 'beaching' during hydraulic deposition. The joints are generally persistent and largely independent of the continuity of filling. Furthermore, close inspection shows these joints to be cohesionless. Inspection of horizontal exposure failure profiles shows the fill to fracture along these joints like that shown in the photographs presented in Figure 4. These joints are expected to make a significant contribution to the paste failure mechanism during horizontal exposures as their orientation make them amenable to separation and sliding when the fill mass is exposed along a (horizontal) plane parallel to the joint orientation. This jointing is not considered in the Mitchell and Roettger (1989) analytical solutions, nor was it considered in the centrifuge testing used to verify their analytical solutions. It is this author's opinion that this jointing fundamentally controls the mechanics of horizontal exposures and, as illustrated in the case studies presented, ignoring the influence of these joints provides a misleading representation about the performance during horizontal exposures.

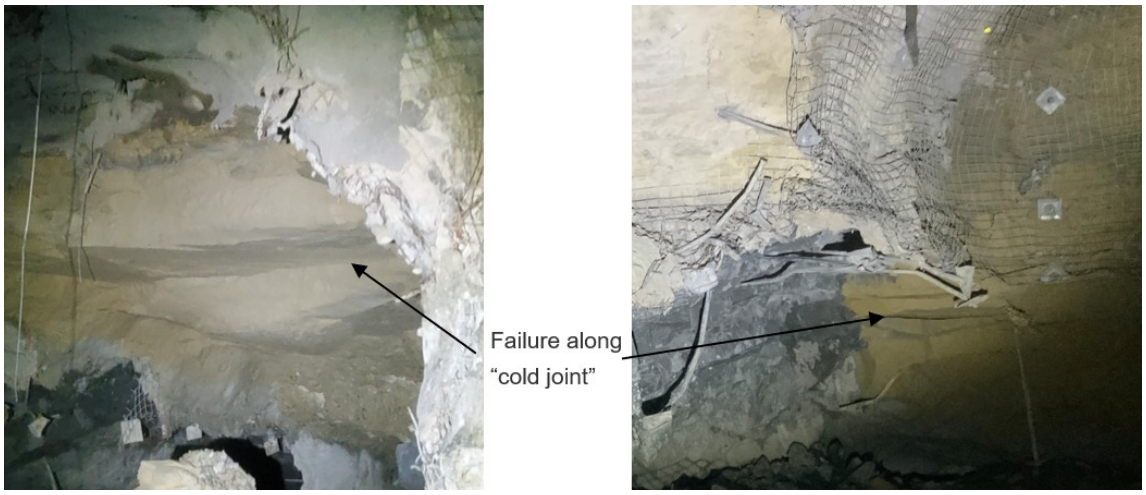

Figure 4. Photographs showing paste backfill failure along cold/flow joints

Numerical Analysis Methodology

Model Geometries

To account for the influence of the jointing when simulating horizontal backfill exposures, analysis was undertaken using a discontinuum Flac3D model (Itasca, 2005), where the cold/flow joints are represented using a series of interfaces. Based on field observations, these joints are typically spaced at 500–750 mm vertical intervals. To represent the jointing interface, horizontal layers are inserted at 625 mm vertical spacing. These interfaces are assumed to possess no cohesion or tensile strength but are assumed to possess the same frictional properties as intact backfill. The quarter-numerical mesh space (ie, symmetry in both vertical planes) with interfaces is presented in Figure 5a, while the deformed mesh is presented in Figure 5b. To represent the stress applied from the overlying fill masses a uniformly distributed surcharge stress was applied to the top of the 'stope scale' model (Figure 5b). This approach reduces the model size requirements. The other notable aspect about these models is that the backfill mass has been extended beyond the exposure such that backfill runs across the abutment.

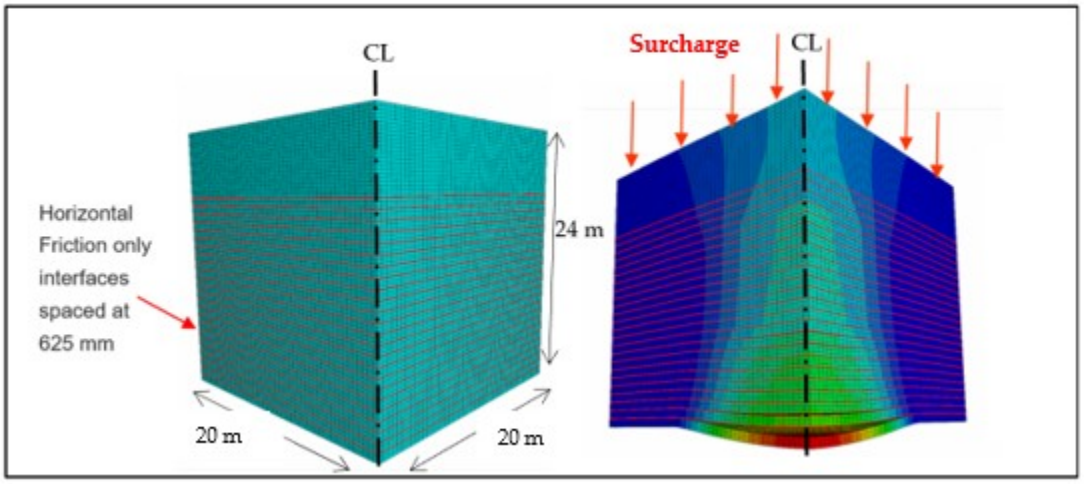

(a) (b)

Figure 5. Numerical discontinuum model uses to simulate horizontal exposures using a) symmetrical, and b) deformed mesh spacing.

In addition to the base case model, consideration was also given to the strength required to sustain various over broken shapes, with the aim of developing a relationship between overbreak (dilution) and backfill strength. It should be noted that in all cases a high strength layer was placed in the lower 15 m of the fill mass and this was overlayed by a low strength fill layer. The low strength layer was set to properties representative of backfill with UCS of 100 kPa, while the strength of the lower layer was iterated. Examples showing the over broken quarter-space models are presented in Figure 6. These models all incorporated the interface layers shown in Figure 5. For each of these model geometries, the backfill strength was progressively reduced until the model geometry became unstable.

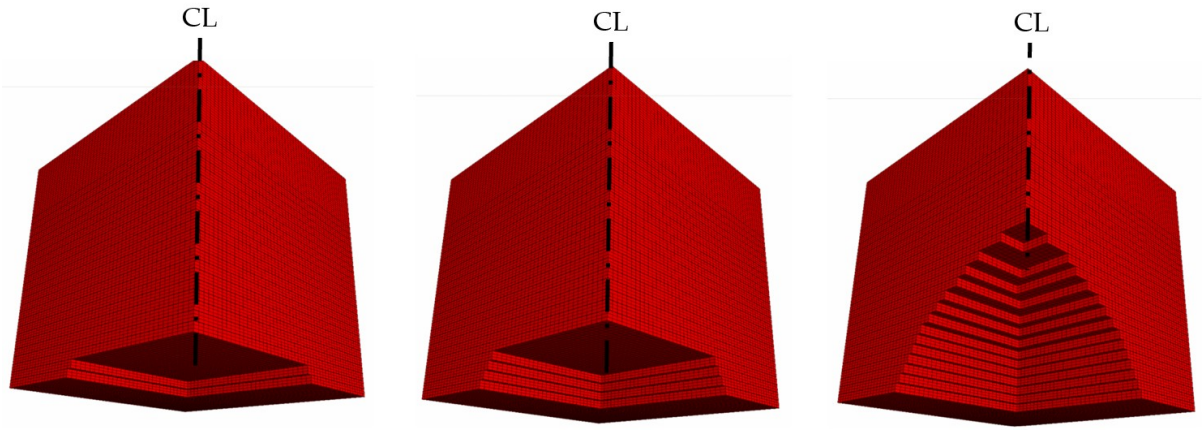

(a) (b) (c)

Figure 6. Quarters space models used to represent overbreak of a) 1.5 m, b) 2.5 m, and c) 12 m.

Model Verification

To assess the performance of the model, field surveys from a number of different horizontal exposures were compared with the modelling results. This back analysis considered two sites, where site paste backfill plant quality control testing was used to determined paste strengths, and stope surveys were used to determine the exposure geometry and overbreak.

Adopting the modelling methodology described above and a representative paste constitutive model (including a Mohr-Coulomb yield surface, with tensile cut-off and post yield strain softening) analysis was undertaken to develop a relationship between strength and overbreak. The calculated relationship between paste strength and depth of failure for a 24 m tall paste mass, exposed over a 24 m × 24 m span, is presented in Figure 7. Superimposed over this plot are field data from similar sized horizontal exposures of fill at two different sites. Results show significant strengths required to maintain no failure. However, these results also show that, if permitting some dilution is acceptable, the strength requirement can be reduced greatly. The RHS of the trend shows the paste strength plateauing while the depth of failure increaes rapidly, indicating that this is a critical strengths below which uncontrolled caving of the fill mass would be occuring.

Figure 7 also shows a good correlation between the numerical relationship and that observed at different sites with similar exposure geometries, with smaller exposures showing a lower failure depth and larger exposures showing greater depth of failure for a given strength. This favourable comparison provides confidence that the proposed approach is valid and is likely to be capturing the failure mechanism appropriately.

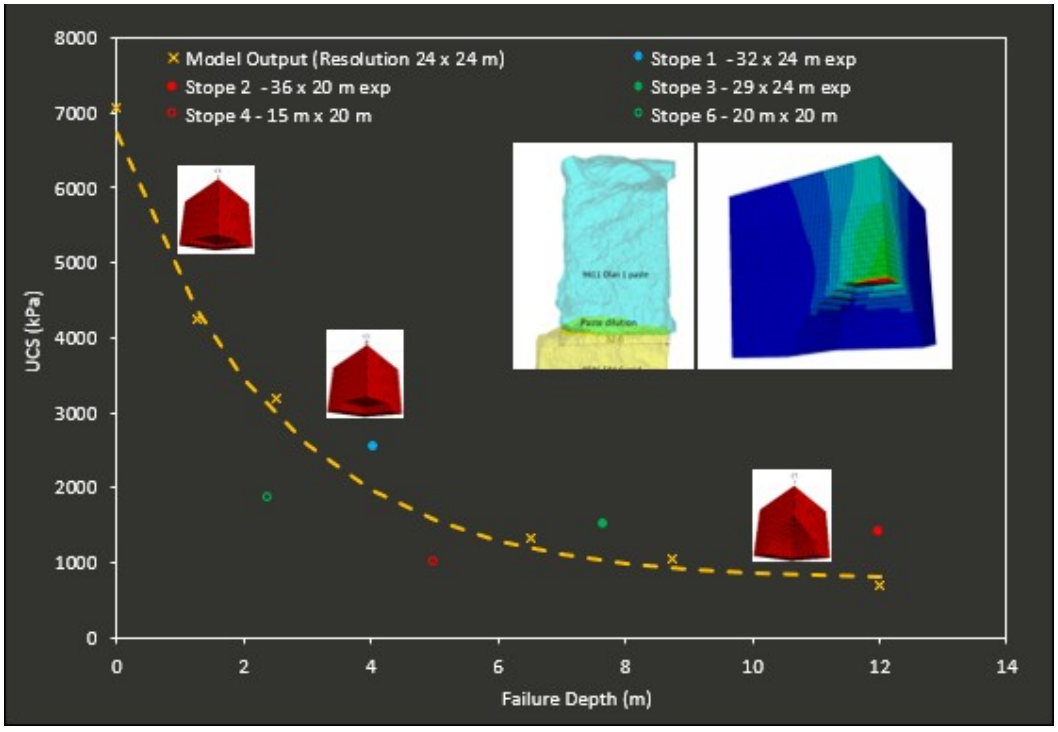

Figure 7. Strengths vs overbreak from modelling results and previous field measurements.

As part of the numerical analysis, consideration was also given to a range of different surcharge stress levels superimposed over the fill mass (as per Figure 5b). For this analysis, consideration was given to the case where all geometries remain the same and only surcharge stresses of 925 kPa and 1400 kPa are applied to the surface of the model (to represent overlying fill). The relationship between failure depth and strength for the various levels of stress are compared with the base case in Figure 8, where analysis results show that the increase in surcharge stress has no influence on the strength required to eliminate dilution (ie. failure depth of 0 m). However, the results show that increasing overburden stress increases the strength required to prevent uncontrolled unravelling of the fill mass. The mechanism controlling this behaviour is described towards the end of this paper.

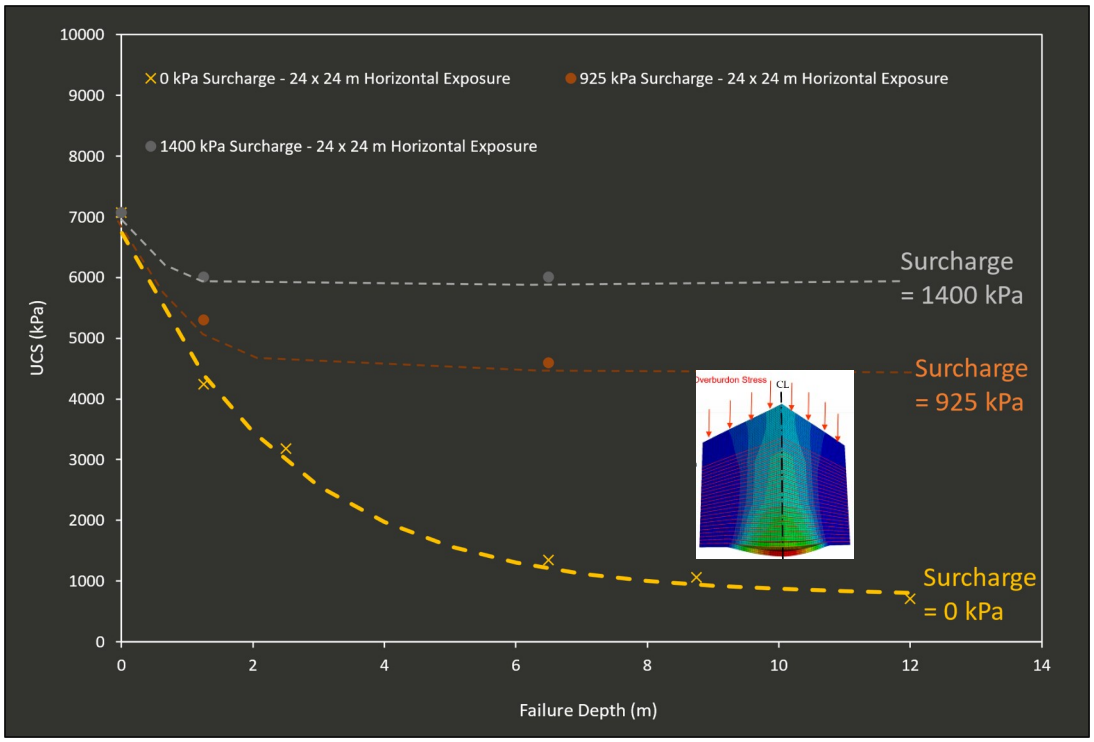

Figure 8. Strengths vs overbreak failure depth with different surcharge stress.

Analytical Solution

Exposure Mechanics

To understand the mechanics of the problem, a detailed assessment of the modelling output was considered. The relevant model output is presented in Figure 9, which shows a cross section through the centre of the fill mass after a horizontal exposure showing only the LHS of symmetry. Figure 9a presents the location of the horizontal cohesionless jointing (pink layers) and displacement contours, where red is maximum, and blue is minimum. Figure 9b presents the backfill tensile strength. As a (tensile) strain softening model is adopted, application of tensile stress that exceed the tensile strength causes a reduction in tensile strength (ie, initially all material has the same strength but zones exposed to excess tensile stress will lose tensile strength). Therefore, (blue) zones representing those with low tensile strength in Figure 9b have yielded in tension. However, it should be noted that a lower strength layer was placed in the upper 9 m of the fill mass. Assignment of this low strength rather than tensile softening explains the low tensile strength (blue zone) in the upper section of the fill mass.

Figure 9c presents the major principal stress contours, where blue/green is the highest and red is the lowest. This section shows where high compressive stresses are forming after the exposure. It should also be noted that in the legend, this is presented as 'Minor principal stress' because the software convention has compressive stress being negative. Also presented in Figure 9c is the major principle stress tensors, which show the orientation of the maximum compressive stress in different zones.

The model output presented in Figure 9a shows displacement discontinuity across the interfaces, illustrating that slippage is occurring across the joints. Figure 9b shows that at the centre of the span zones, the base of each layer (ie, immediately above each interface joint) has lost all tensile strength while the abutment has also lost tensile strength. This suggests that each layer is yielding in accordance with the 'flexural' failure mechanism.

However, as discussed by Grabinsky and Jafari (2015), after tensile yielding occurs kinematic rotation causes a compressive 'stress arch' to form within each layer. This is illustrated in Figure 9c where the high (negative = compression, green contours) stress forms in the upper zones at the centre of each layer and in the lower zones of each layer at the abutment. The stress arch shape is also shown by the location and orientation of major principal stress tensors that are superimposed over Figure 9c.

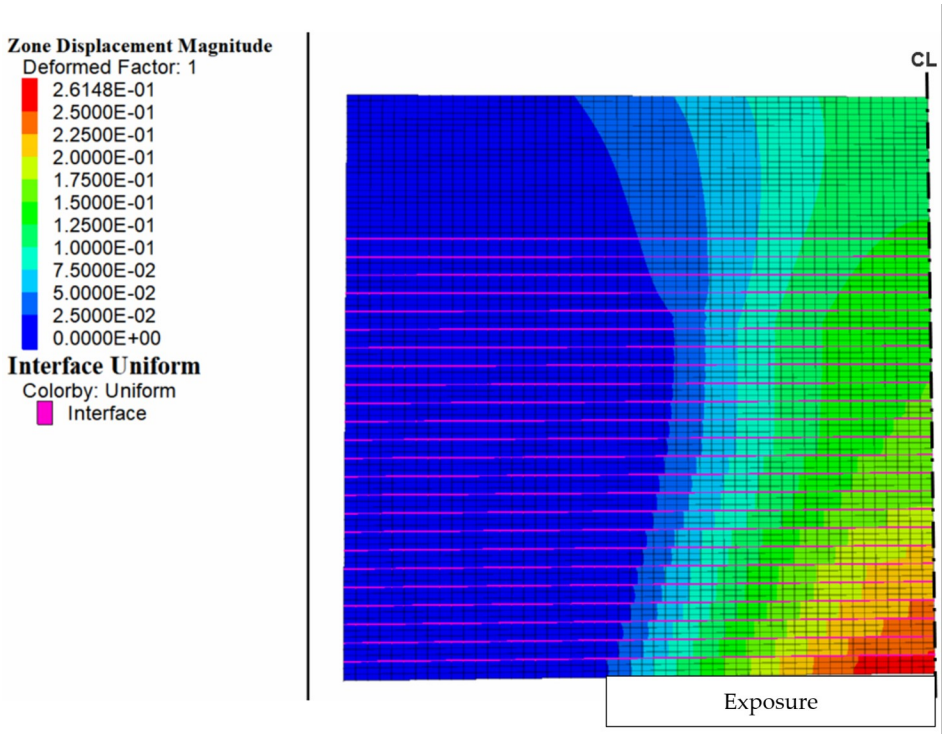

a)

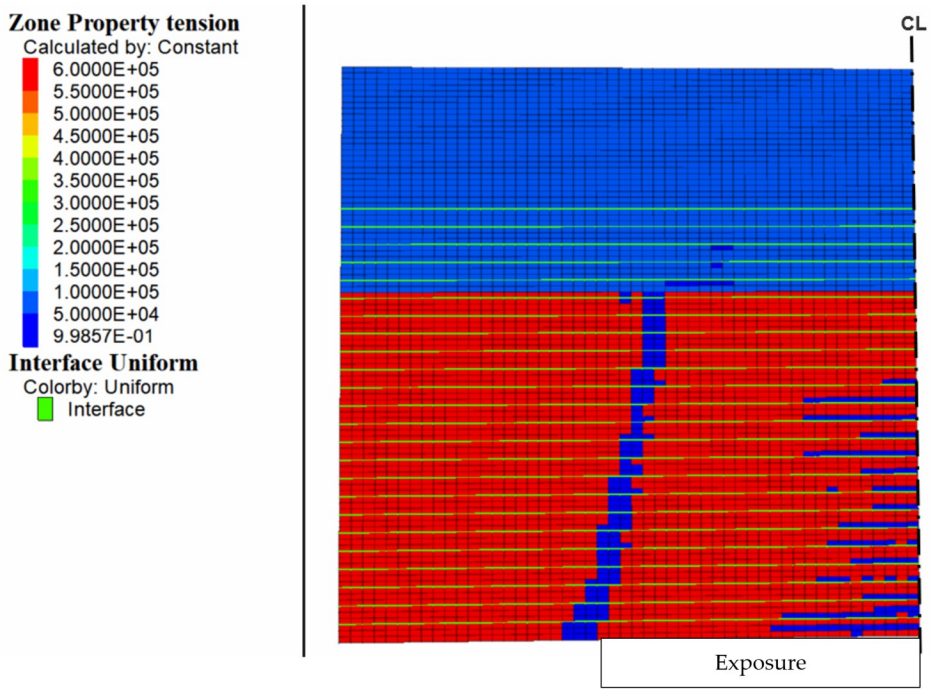

(b)

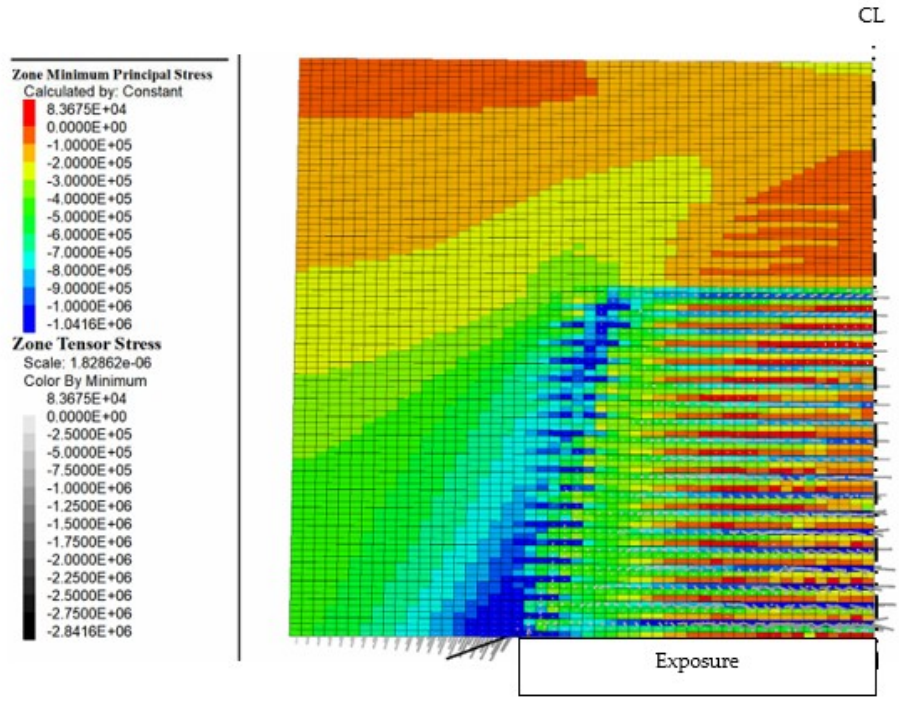

(c)

Figure 9. Model section showing mode output for a horizontal exposure with cohesionless interfaces showing: a) displacement, b) tensile strength, and c) major principal stress.

This stress regime shows each individual beam forming a compression arch. Detailed review of the numerical output shows that the beams remain stable until the compressive stress in each beam exceeds the strength. This mechanism was previously introduced by Grabinsky and Jafari (2015) where they developed a 'strut and tie' model to represent the behaviour. The approach taken in this paper is similar, but uses the "Voussoir beam" analytical model, which is discussed in the following section. The other notable aspect about Figure 9b is the high stress concentration at the abutment of the exposure, where the fill mass stress is redistributed around the opening and into the abutments. This mechanism can be represented using Kirsch's (1898) solution for stress redistributed around a circular opening and is discussed further towards the end of this paper.

Voussoir Beam Analytical Model

Limit Equilibrium

The Voussoir beam model is shown schematically in Figure 10a, with the compressive stress distribution shown in Figure 10b. These images are taken from Diederichs and Kaiser (1999), where a complete description of this mechanism is provided.

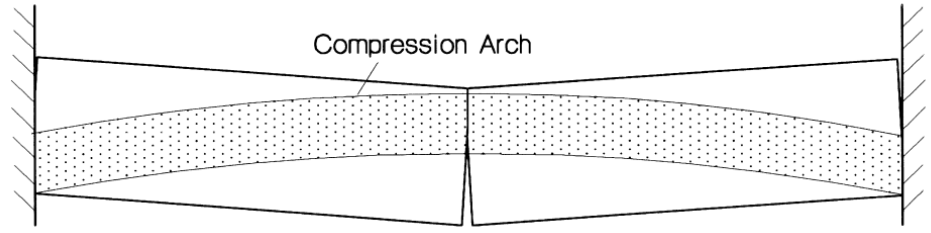

(a)

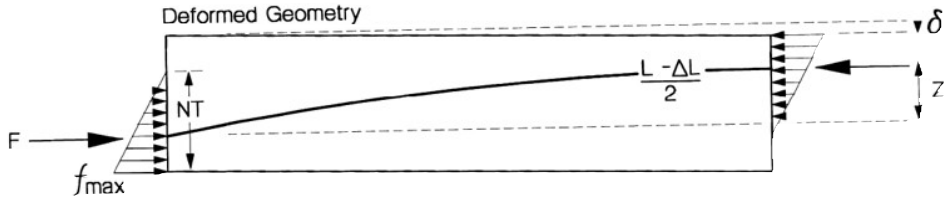

(b)

Figure 10. Illustration showing the Voussoir beam mechanism (from Diederichs and Kaiser, 1999).

Using this mechanism, Diederichs and Kaiser (1999) derive a function to relate the approximate beam strength (*UCS*) requirements to support a confined beam, of thickness *T*, over span *S*, under self-weight conditions with unit weight, γ (Equation 1).

$$UCS \approx \frac{\gamma . S^2}{4 . N . T \left(1 - \frac{2}{3} N\right)} \qquad \text{Equation 1}$$

where *N* is a constant that (with reference to Figure 10b) is controlled by the shape of the arch forming within the beam.

For stable beams Diederichs and Kaiser (1999) suggest that *N* can range from 0.3–0.7, where the appropriate value is dependent on the span to beam thickness ratio and material stiffness. Typical backfill exposures would have a high span to thickness ratio and relatively low stiffness, suggesting that an appropriate *N* value would be towards the lower end of the range. To provide a comparison with the Voussoir beam theory and the numerical approach, plane-strain numerical analysis was undertaken using a constitutive model representative of typical backfill and the interface model described in relation to Figure 5. This analysis considered plane strain spans of 8, 16 and 24 m to determine the minimum strength requirements for stability. Analytical results are presented as symbols in Figure 11. Superimposed over these data is Equation 1, using a beam thickness of 625 mm, a unit weight of 20 kN/m^3 and an *N* factor of 0.4. Diederichs and Kaiser (1999) note that, after initial deformation, each beam transfers its own weight to the abutment rather than loading the beam beneath; as such, it is not necessary to consider a surcharge load in the Voussoir beam analysis.

Comparison between the numerical and analytical solution presented in Figure 11 show that, with an *N* factor of 0.4, the numerical and analytical solutions provide a similar relationship; also presented is the three-dimensional numerical solution for a 24 m × 24 m span. This comparison shows that the three-dimensional influence is very significant and for accurate results should be taken into consideration.

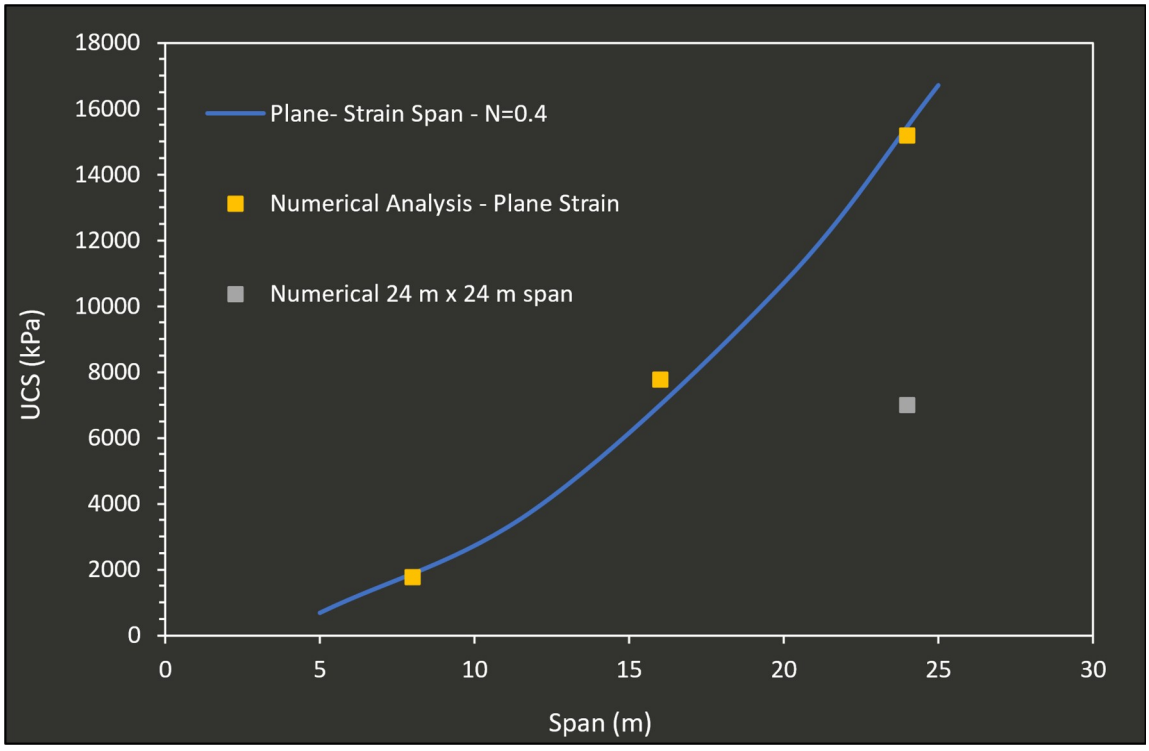

Figure 11. Comparison between strength definition using Voussoir beam theory and that from numerical analysis.

Dilution Estimates

While the analysis results presented in Figure 11 show the strength requirement to be very high (if aiming to eliminate dilution), experience shows that, in practice, the fill tends to unravel in layers with the progressive layer breaking off closer to the centre of the span to create a lesser span for overlying layers.

This is illustrated in the surveys presented in Figure 2 and photograph of an unravelled fill mass presented in Figure 4. As the fill unravels the reduction in span enables stability to be achieved, with lower strength backfill requiring further overbreak for stability. In many cases, the consequence of failure is limited to this increased dilution, which may be tolerable.

Based on survey information from horizontal exposures and the stress distribution in numerical analysis, it is considered reasonable to idealize overbreak around horizontal exposures to break back at an angle of approximately 45°. With this assumption, the over broken geometries and resulting spans are presented in Figure 12.

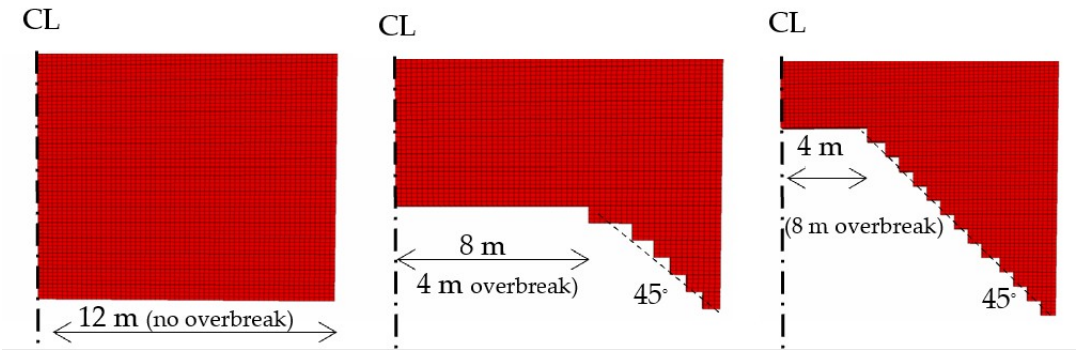

Figure 12. Modified geometries after dilution.

Using the geometries presented in along with the same constitutive model and interface arrangement described previously, numerical analysis was undertaken to determine the strength requirements to maintain stability of the (initial) 24 m plain strain geometries, but allowing for this overbreak. The results from this analysis are compared with the Voussoir beam function and the smaller span numerical results in Figure 13.

This comparison shows that, even though the initial span is 24 m in all cases, after allowing for the reduction in span that comes about after some dilution (ie, open symbols), the strength required to maintain stability of the over broken geometry can be approximated by the horizontal exposure span created after the overbreak.

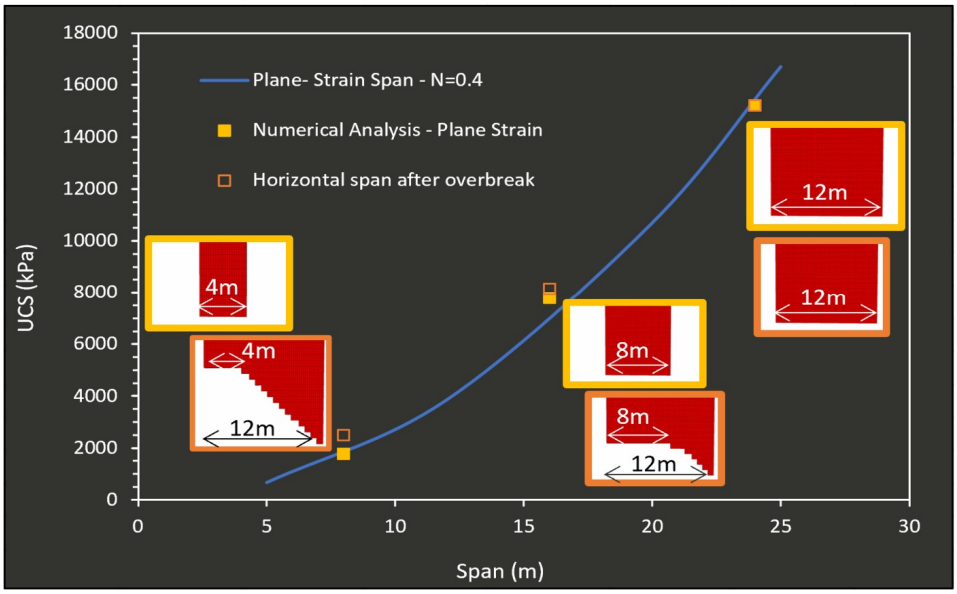

Figure 13. Comparison between strength required for complete span and that required to sustain the over-broken span.

Using this logic, the Voussoir beam model presented in Equation 1 can be modified to Equation 2, which can then be used to develop a dilution versus strength relationship similar to that generated from numerical analysis (i.e. similar to Figure 7):

$$UCS \approx \frac{\gamma . \left(S - \frac{2.Ho}{tan\alpha}\right)^2}{4.N.T\left(1 - \frac{2}{3}N\right)} \qquad \text{Equation 2}$$

where H_o is the height of overbreak, α is the average angle that the backfill over breaks from the abutment and the factor controlling the shape of the arch forming in a beam (N) could be approximated as 0.4. Figure 14 provides a schematic to illustrate the assumed overbreak geometry and model parameters. The author's assessment of cavity mine survey information suggests that the average overbreak angle α to be approximately 45°, but this is likely a site-specific parameter.

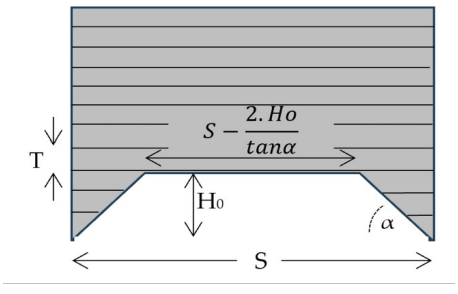

Figure 14. Idealised failure geometry assumed for Equation 2.

Finally, it should be recognised that Diederichs and Kaiser (1999) discuss a "snap-though" mechanism, which occurs when large spans with thin beams of low stiffness material incur elastic deformation that prevent a Voussoir beam from forming (ie, the N term in Equation 1 and 2 approaches zero prior to the onset of yielding). This mechanism may limit the application of the Voussoir beam analytical model for very large spans however further investigation of this mechanism is beyond the scope of this work.

Kirsch's Stress Redistribution

Figure 8 shows that the application of increasing surcharge stress has no impact on the strength required to eliminate dilution, however the surcharge stress results in the need for higher strengths to prevent uncontrolled unravelling (ie, catastrophic failure). The influence of field stress on a horizontal exposure showing the major principal stress in a section through the center of the fill mass is illustrated in Figure 15a and b before and after a horizontal exposure, respectively. Comparison between these two images show that the horizontal exposure creates a very high stress concentration at the abutment of the exposure.

Specifically, the model output shows the maximum major principal stress to increase from approximately 700 kPa (prior to the exposure) to approximately 2500 kPa at the abutment (after the exposure). This stress increase is largely independent of any overbreak immediately above the exposure (as described in the previous section). As such, should the fill strength be insufficient to sustain this stress, the failure mechanism would transition from the Voussoir mechanism to one of shear failure at the abutment. Should shear failure occur at the abutment the fill would be unable to sustain the over broken "arch" profile and would unravel uncontrollably, caving with catastrophic levels of dilution. This mechanism is expected to be the reason that the strength versus dilution curves presented in Figure 8 are sensitive to the surcharge stress.

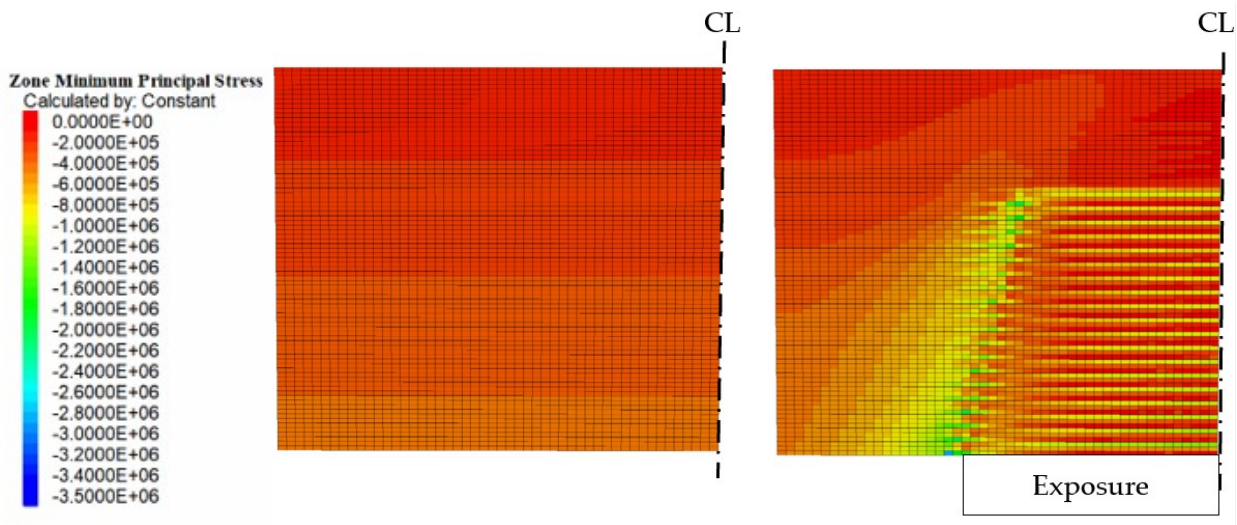

(a) (b)

Figure 15. Major principal stress: a) before, and (b) after an exposure.

To determine the strength at which a stable arch could not be sustained (ie, the fill mass would unravel uncontrollably), Kirsch's (1898) solution for a hole in an infinite medium could be considered. This solution suggests that the maximum stress concentration and the edge of a circular opening may be approximated as three times the (pre-excavation) field stress. Assuming that the failure arch is to form a

circular shape and that fill at the abutment is unconfined, if the fill's unconfined compressive strength is greater than three times the field stress a stable arch would be expected to form. This ratio aligns with the increase in stress (3.5 times increase) shown in Figure 15. The pre-exposure field stress could be determined numerically using a mine scale continuum model or an analytical solution such as that originally proposed by Terzaghi (1943) and applied to backfill the scenario by others (Baldwin and Grice, 2000).

Tensile Strength Sensitivity

The horizontal exposure mechanics presented in this document show that backfill beams located immediately above horizontal exposures tend to fail in flexure (yielding in tension) before rotational kinematics led to formation of a Voussoir arch. As such, dilution is controlled by failure of the Voussoir arch, which is ultimately controlled by compressive strength. Furthermore, another mechanism controlling stability is associated with shearing at the exposure abutments from the increase in stress associated with redistribution of field stress around the exposure. In accordance with these mechanisms horizontal exposure dilution is effectively independent of the fill mass tensile strength.

To investigate this premise, a sensitivity study was undertaken. The model geometry adopted for this study is identical to that for the 16 m plane strain case in the main body of this paper. Analyses presented earlier in the paper assumed the tensile strength to be equal to the fill cohesive strengths. For the sensitivity study, this ratio was modified to consider the tensile strength as being 50%, then 200% of the cohesive strength. With each of these tensile strength ratios, the backfill strength was progressively reduced until failure occurred. Analysis showed that the compressive strength required to maintain stability was the same regardless of the tensile strength ratio adopted.

This study illustrated that, in accordance with the proposed analytical solutions, the horizontal exposure strength requirement is independent of tensile strength.

Conclusion

The author's experience has shown commonly adopted analytical solutions for determining backfill horizontal exposure strength requirements perform poorly when applied to hydraulically placed backfill over large unsupported spans. This poor performance is attributed to the presence of cohesionless 'cold' or 'flow' jointing created within the backfill during the hydraulic deposition process.

Using a combination of numerical analysis and field observations this paper presents a detailed review of the controlling horizontal exposure mechanism, demonstrating that:

- Ignoring the presence of horizontal jointing in hydraulically placed backfill significantly underestimates the backfill strength required to eliminate dilution.
- Due to kinematic constraints, flexure during horizontal exposures is not a destabilising mechanism and rather the failure mechanism for fill immediately overlying a horizontal exposure is (Voussoir beam) crushing.
- Where a limited quantity of dilution is acceptable, stability of large horizontal exposures can be maintained with modest backfill strengths.

Discontinuum analysis is used to develop a relationship between overbreak and backfill strength for a 24 m × 24 m horizontal exposure. This relationship compares favourably with field measurements from five different exposures of similar size at two different sites, which provides confidence that the model is

capturing the correct mechanisms. Given the mechanics observed in the numerical output, Voussoir beam theory appears to provide a reasonable representation of the fill immediately overlying the exposure. A comparison between numerical simulations and the Voussoir beam model show that, with an appropriate arch geometry factor (*N*), the Voussoir beam model presents an excellent tool for estimating the strength required to eliminate dilution during horizontal exposures.

Further analysis examining the stability of backfill after permitting some overbreak showed that (for a given overbreak geometry), the strength requirement is controlled by the effective horizontal span (ie, when accounting for the reduction in span as the overbreak progresses inwards). Based on this finding, a modified version of the Voussoir beam analytical model is proposed, to relate the backfill strength to the overbreak depth.

During horizontal backfill exposures, *in situ* stress is redistributed around the opening to create a stress concentration at the abutment of the exposure. If the backfill has insufficient shear strength to sustain this stress the abutment yields resulting in uncontrolled caving of the fill mass. To account for this stress concentration, Kirsch's (1898) solution for a hole in an infinite medium is proposed. This solution suggests that a stress concentration equal to three times the pre-exposure stress would be created at the abutment of a circular opening. Provided that the backfill unconfined compressive strength exceeds this value, the backfill is expected to form a stable arch shape.

Finally, given that the mechanics controlling the horizontal exposure stability are dictated by compressive rather than tensile stress, a numerical sensitivity study was undertaken to assess the sensitivity of tensile strength to the analysis results. The results showed that either a 50% reduction or 100% increase in tensile strength had no influence on backfill strength requirements for a given horizontal exposure.

References

Baldwin, G. and Grice, A.G. (2000) Engineering the New Olympic Dam Backfill System, Proceedings Massmin,Australian institute of Mining and Metalurgy, pp. 705-711.

Diederichs, M.S. and Kaiser, P.K. (1999) Stability of Large Excavations in Laminated Hard Rock Masses: The Voussoir Analogue Revisited. International Journal of Rock Mechanics and Mining Sciences, 36, pp. 97-117.

Grabinsky, M., Jafari, M. and Pan, A. (2022) Cemented Paste Backfill (CPB) Material Properties for Undercut Analysis, Application of Empirical, Analytical and Numerical Approaches in Mining Geomechanics, Mining, ISSN 2673-6489

Grabinsky, M. and Jafari, M. (2015) Determining stable spans of undercut cemented paste backfill, GeoQubec 2015.

Itasca Consulting Group, Inc. (2005) FLAC3D (Fast Lagrangian Analysis of Continua in 3D), Version 3.0 Minneapolis: ICG.

Kirsch, E.G. (1898). *Die Theorie der Elastizität und die Bedürfnisse der Festigkeitslehre".* Zeitschrift des Vereines deutscher Ingenieure, Vol. 42, pp. 797-807

Mitchell R.J. and Roettger J.J. (1989) Analysis and modelling of sill pillars. Innovations in mining backfill technology. Balkema, Rotterdam, pp 53–62

Pakalnis, R.; Caceres, C.; Clapp, K.; Morin, M.; Brady, T.; Williams, T.; Blake, W.; MacLaughlin, M. Design Spans-Underhand Cut and Fill Mining. In Proceedings of the 107th CIM-AGM, Toronto, ON, Canada, April 2005; pp. 1–9.

Terzaghi, K.V. (1943) Theoretical Soil Mechanics, P510, John Wiley:New York